Luttinger Liquids

Michelle Nahas

Emergent States of Matter
May 06, 2002

Abstract

Luttinger liquids are paramagnetic one-dimensional metals that do not exhibit the quasi-particle excitations of Fermi liquid theory. Rather Luttinger liquids will be seen to have strong responses to any perturbation no matter how small. Bosonization will be used to expand the Fermi fields in terms of boson operators, allowing almost all physical properties to be calculated. It will be seen that the correlation function exhibits power law behaviour which leads to the experimental prediction of power law conductance for tunnelling into Luttinger liquids. The results of experiments that measure the tunneling conductance of by electrostatic force microscopy (ESM) on single walled carbon nanotubes will then be discussed and compared to these predictions.

1 Introduction

The ground state of an interacting one dimensional electron gas is a strongly correlated state known as a Luttinger liquid. The signature behaviour of Luttinger liquid systems are spin charge separation and power law behaviour of the correlation functions. The theory of such systems was worked out independently in the condensed matter and high energy communities by Luttinger and Tononaga several decades before any experimental evidence existed.

The behaviour of Luttinger liquids is strikingly different from that observed in two and three dimensional systems of interacting Fermions. Such systems obey Fermi liquid theory down to very low energies. In these higher dimensions scattering of the quasiparticle exciations described in usually destroys the Fermi liquid phase only through spontaneous symmetry breaking on an energy scale T_c which is orders of magnitude below the Fermi energy. In 1 D, Fermi liquid behaviour never develops, all perturbations to the noninteracting Fermi gas have large effects.

In this paper a brief overview of the theory of Luttinger liquids is first developed. The main emphasis being the prediction of two characteristic properties of Luttinger liquids mentioned above. This theory is then used to compare to experimental results obtained through conductance experiments performed on single walled carbon nanotubes (SWNT) [6].

2 1D is special

In 1D a very elegant simplification in the description of the excitation spectrum for the fermi gas can be made. From Fig. 1a. it can be seen that for any small energy excitation above the 1D fermi surface, the momentum vectors of the particle and hole must point in the same direction. Hence the excitation leads to a coherent particle hole pair. Any weak particle hole interaction will then have drammatic effects essentially binding the pair into a coherently propagating entity, a new particle.

Such coherent behaviour of fermi surface excitations is not required in 2D and 3D. In these higher dimensions a small energy excitation can correspond to a continuum of possible k vector excitations. This can be seen in figure 1b where the open circles represent possible k vector values describing the hole produced be the solid circle particle excitation.

Because of this coherence of excitations in 1D the fermi wavefunctions and corresponding hamiltonian can be rewritten in terms of boson operatorswhich will be discussed below.

2.1 Noninteracting Electrons in 1D

Noninteracting fermions in 1D can be described by a Hamiltonian of the form

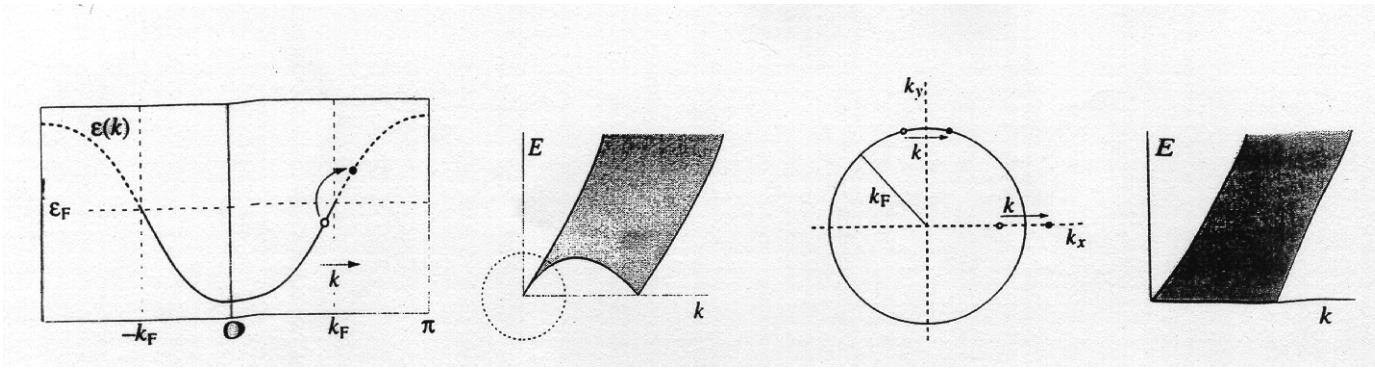

Figure 1: 1a) Particle hole excitations are shown for 1D excitations. 1b) Particle hole excitations shown for 2D excitations

$$H_F = \int \frac{dk}{2\pi} v|k|\{\alpha(k)^\dagger \alpha(k) + \beta^\dagger(k)\beta(k)\} \tag{1}$$

where the expansion is in terms of particle and hole operators at the fermi surface, meaning for example that the operator $\alpha(k)$ destroys particles of momentum $k+k_f$.

The mode expansions for continuous fermion fields can then be written in terms of left and right separated components

$$\psi_R = \psi(z) = \int_{k>0} \frac{dk}{2\pi}[e^{-kz}\alpha(k) + e^{kz}\beta^\dagger(k)] \qquad \psi_L = \psi(\bar{z}) = \int_{k<0} \frac{dk}{2\pi}[e^{k\bar{z}}\alpha(k) + e^{-k\bar{z}}\beta^\dagger(k)] \tag{2}$$

Where the expansion has been written in terms of $z = x+iv|k|t$ (left moving) and $z = x - iv|k|t$ (right moving). For a system of noninteracting bosons the expansion is almost identical to (2) except there are no commutation relations between the particle hole creation destruction operators.

$$\phi_R = \phi(z) = \int_{k>0} \frac{dk}{2\pi}[e^{-kz}b(k) + e^{kz}b^\dagger(k)] \qquad \phi_L = \phi(\bar{z}) = \int_{k<0} \frac{dk}{2\pi}[e^{k\bar{z}}b(k) + e^{-k\bar{z}}b^\dagger(k)] \tag{3}$$

2.2 Bosonization

Considering that the excitation spectrum for 1D Fermi metals behaves as a collection of Bose an ansatz[3] for the boson representation of the fermi field is proposed

$$\psi^\dagger(z) = Ae^{2i\lambda\phi(z)} \qquad \bar{\psi}^\dagger(z) = Ae^{2i\lambda\bar{\phi}(z)} \tag{4}$$

The ansatz is written in terms of fermion creation operators so that when $psi^\dagger$ operates on the vacuum a one electron state state is generated by exponentials of boson operators and hence has the desired property of being a coherent state. The constants A and λ can be determined by comparing the Green functions calculated from the free fermion wave functions in (2) to the one calculated from (4).

$$< \psi(z)\psi^\dagger(z') >= \frac{1}{2\pi(z-z')} = \frac{A}{(z-z')^{-\lambda\frac{2}{2\pi}}} \tag{5}$$

Fixing the constants as $\lambda = \sqrt{\pi}$ and $A = \frac{1}{\sqrt{2\pi}}$. The correct bosonization formulas are then

$$\psi^\dagger(z) = \frac{1}{\sqrt{2\pi}}\eta e^{-i\sqrt{4\pi}\phi(z)} \qquad \bar{\psi}^\dagger(z) = \frac{1}{\sqrt{2\pi}}\bar{\eta}^{i\sqrt{4\pi}\bar{\phi}(z)} \tag{6}$$

The Klien factors, η, are included so that the fermion fields obey the proper anticommutations results. $\{\eta_\mu, \eta_\nu\} = \{\bar{\eta_\mu}, \bar{\eta_n}u\} = 2\delta_{\mu\nu}$.

Before considering interactions are considered spin is introduced. Writing the left and write separated free boson fields in terms of $\varphi(x)$ as $\varphi(x,t) = \phi_R + \phi_L$. Then the fields $\varphi_\uparrow$ and $\varphi_\downarrow$ are definedas

$$\varphi_c = (\varphi_\uparrow + \varphi_\downarrow)/\sqrt{2} \qquad \varphi_s = (\varphi_\uparrow - \varphi_\downarrow)/\sqrt{2} \tag{7}$$

In terms of these new boson fields as the Hamiltonian to split into independent "spin" and "charge" fields. For instance the right moving fermion field in (6)

$$\psi_{R\uparrow} \propto e^{i\sqrt{4\pi}(\phi_{cR}+\phi_{sR})} \qquad \psi_{R\uparrow} \propto e^{i\sqrt{4\pi}(\phi_{cR}-\phi_{sR})} \tag{8}$$

2.3 Luttinger Liquid Model

To obtain Luttinger liquid behaviour the effect of interactions must be included. The theory will be obtained in the low energy excitation limit, ie excitations near the Fermi surface. Scattering processes in this limit fall into four kinematic types. These possible interactions are sumarized in Fig. 2a. The free and bosonized forms of these interaction Hamiltonians are listed in Fig. 2b and Fig. 2c respectively.

From the form of the interaction terms in Fig. 2 it can be seen immediately that when only the g_2 and g_4 types of interactions are present is it possible to express the interacting Hamiltonian as a free Hamiltonian with the fields rescaled by the parameter K_μ below. The Hamiltonian with only H_2 and H_4 interactions present forms the Luttinger-Tomonaga model.

$$H_L = H_{free} + H_{2,c} + H_{2,s} + H_{4,c} + H_{4,s} \tag{9}$$

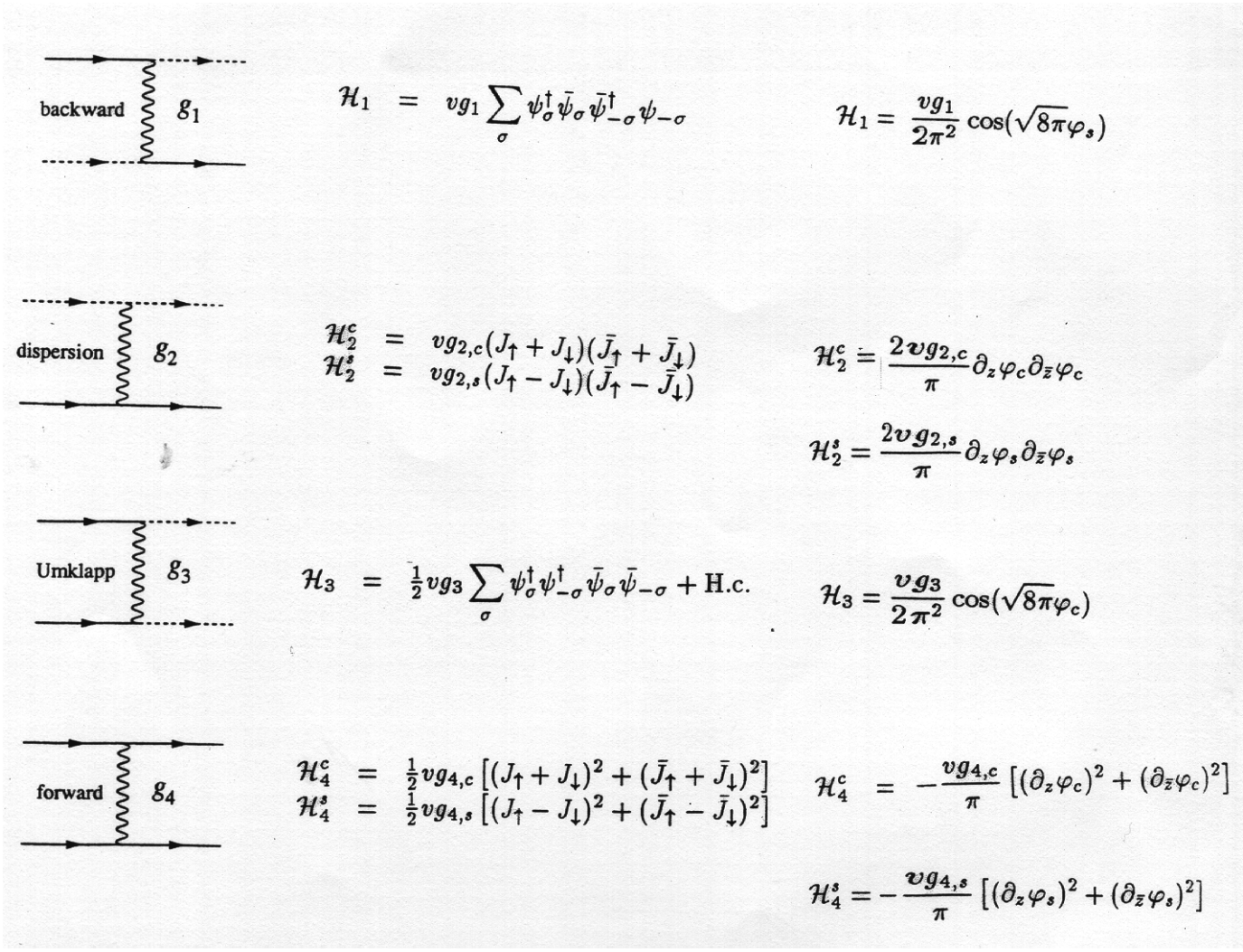

Figure 2: The four possible scattering processes for right-moving (continuous line) and left-moving (dashed line) electrons in one dimension. Spin indices have been suppressed. Where $J_\uparrow = \psi^\dagger(x)\psi(x)$, $\bar{J}_\uparrow = \bar{\psi}^\dagger(x)\bar{\psi}(x)$, are the right and left electron density fluctuations respectively. Denoting the charge spin components by μ the total interaction Hamiltonian is then $H_L = H_f + H_1 + H_{2,\mu} + H_3 + H_{4,\mu}$.

Substituting the bosonized expressions for H_2 and H_4 from Fig. 2 into (9) using the following relations and the index μ to denote charge and spin modes

$$\Pi_\mu = \frac{1}{v_\mu}\partial_t\varphi_m u \quad \partial_z = \frac{-i}{2}(\frac{1}{v}\partial_t - \partial_x) \quad \partial_{\bar{z}} = \frac{-i}{2}(\frac{1}{v}\partial_t + \partial_x) \tag{10}$$

The Hamiltonian can then be simplified by grouping terms into

$$H_\mu = \frac{1}{2}v_\mu[K_\mu {\Pi_\mu}^2 + \frac{1}{K_\mu}(\partial_x\varphi_\mu)^2] \tag{11}$$

$$K_\mu = \sqrt{\frac{\pi - g_{2,\mu} + g_{4,\mu}}{\pi + g_{2,\mu} + g_{4,\mu}}} \qquad v_\mu = v\sqrt{(1 + \frac{g_{4,\mu}}{\pi})^2 - (\frac{g_{2,\mu}}{\pi})^2} \tag{12}$$

As for the interactions H_3 and H_1 from their expressions in Fig. 2 it can be seen that inclusion of theses will add the equivalent of a mass term to the Hamiltonian. Like the addition of mass to any free field this will lead to effective charge and spin gaps in the energy spectrum. These terms will not be considered furthur.

From the form of the Luttinger Hamiltonian (11) all correlation functions can be calculated as simple harmonic oscillator averages. This can be done by repeatedly using the identities: $< e^A >= exp(< A^2 > /2)$ and $e^A e^B = e^{A+B}e^{[A,B]/2}$.

Using this procedure the one particle Greens function can be calculated. In terms of the particle hole operators it can be written as

$$G_\uparrow =< \psi_\uparrow(x,\tau){\psi_\uparrow}^\dagger(0,0) > + < \bar{\psi_\uparrow}(x,\tau){\bar{\psi_\uparrow}}^\dagger(0,0) > \tag{13}$$

Considering only the right-moving part in the case $K_s = 1$ and $K_c \neq 1$ and using the identities mentioned above after a little manipulation (1)

$$< \psi_\uparrow(x,\tau){\psi_\uparrow}^\dagger(0,0) >= \frac{1}{2\pi}\frac{1}{(v_c\tau - ix)^{1/2}}\frac{1}{|v_c\tau - ix|^\alpha}\frac{1}{v_s\tau - ix)^{1/2}} \tag{14}$$

Where τ is it and

$$\alpha = \frac{1}{4}(K_c + \frac{1}{K_c} - 2) \tag{15}$$

The Greens function has power law singularities near ω_s and ω_c with exponent α. This power law scaling is distinctly different from the results of fermi liquid theory. Here arbitarily small perturbations to the hamiltonian always have significant effects. Taking the Fourier transform of the Green function it can be shown

$$n(k) \propto |k - k_f|^\alpha \tag{16}$$

The density of states which is related to the tunnelling current is then expected to exhibit scaling behaviour dependent on the exponent α. Note the differece of this result as compared to the prediction of Fermi liquid theory that α=0. In the next sections the results of experiments measuring this parameter will be discussed.

3 Carbon Nanotubes

To date the cleanist experimental observations of Luttinger liquid behaviour have been established through transport properties of single wall nanotubes (SWNT). [7] In contrast to conventional systems, semiconductor quantum wires, Luttinger liquid effects in SWNT are not restricted to the meV range but may be seen at room temperature. SWNT are 2D graphite sheets that are folded with no overlap of the sheet into a cylinder. The vector (N,M) shown in Fig.3 is used to completely characterize the nanotube. This vector indicate which 2 hexagons will be connected along their edge when the sheet is folded, thus determining the radius and chirality of the tube. The existence of carbon nanotubes bandstructure is due to the confinement of electrons normal to the nanotube axis. The conducting electrons then can propagate with quantized energies along the direction parallel to this axis. SWNT may be metallic or semiconducting depending on the rolling vector chosen. For the systems studied below only (N,N) nanotubes will be considered which are known to be metallic. Though experimentally single tubes are not deposited rather bundles of tubes are, but it has been found that the conduction in such bundles is dominated by a single metallic tube[6]. The others are semiconducting and hence insulators at low temperatures.

Before the theoretical treatment is undertaken it should be stated that metallic SWNT will be considerd to behave as ballistic conductors, meaning there is no scattering within the conductor. Such behaviour is observed through electrostatic force microscopy (EFM) [3]. The set up for EFM is shown in Fig. [3.1]. It is a technique that measures elecrostatic force through the bending of an AFM tip towards or away from a surface. The EFM technique will be described here since it will be described in Sec. 3.1 as it is the technique used to measure the conductance of the nanotubes in the main experiments discussed below. The analysis in the following section will take this viewpoint though it should be noted that other experiments [7] support the model of the bulk nanotube being a dispersive conductor. Using the ballistic conductance model, measurements on these nanotubes can be interpretted as due only to events at the junction of the nanotube-probe. But this then depends on the ability of electrons to tunnel from the probe (Fermi liquid) into the nanotube and hence on the density of states near the tunnelling energy.

The SWNT will be treated as a 1D Fermi gas with a Coulomb interaction which will lead to a Luttinger model with only the forward scattering interaction term of Fig. 2 included. This simplification is justified for nanotubes described by large N. This is justified because interbranch scattering (backscattering and umklapp) involve momentum transfers of $2k_f \sim 1/a$, where a is the carbon-carbon bond length. Such terms describe the short range part of the interaction which changes significantly from site to site. Howerver the electrons in the lowest subband are spread over the circumference of the tube, and for large N the probability of two electrons being

near eachother will be small. By contrast forward scattering processes in which electrons stay in the same branch will involve small momentum exchange. They are dominated by the long range part of the coulomb interaction. The dispersion term is neglected since it couples states moving in opposite direction whereas for the conducting state that the model aims to derive this term should be negligible. So considering only forward scattering leads to only the $H_{\mu,2}$ term being nonzero in the interaction Hamiltonian of Eqn[9].

But before a direct analogy is made between the previous analysis the degeneracy due to the electron spin and the sublattice in the SWCT must be included. Each of these symmetries adds two degeneracies to the original system giving four possible modes for each channel contained in parameter μ. Considering only the long range part of the interaction $V_0(x-x') = \int V(k) e^{k(x-x')}\ V_0(k\ 0)$.

The tunnelling density of states can be obtained from the previous result Eqn.(16) noting that in 1D $dE \propto dk$.

$$\rho(E) \propto E^{\alpha} \tag{17}$$

Where α is given by the end tunnelling exponent given in Eqn.(15). Though experimentally there will be a correction to this formula depending on the way in which the nanotube is connected to the probe which will be discussed below. The expression for α depended on the parameter K_0 which in this section will be renamed g, as it now pertains to the SWNT system. Substituting into Eqn. (12) taking into account the four fold degeneracy and setting and $g_{4,\mu} = \frac{V_0(k\ 0)}{\hbar v_f}$ and all other $g_{1,\mu} = 0$:

$$g = (1 + \frac{4V_0(k\ 0)}{\pi \hbar v_f})^{-1/2} \quad = (1 + \frac{2E_c}{\Delta})^{-1/2} \tag{18}$$

The second equality in Eqn.(18) comes from the mean level spacing $\Delta = hv_f/4L$ and the charging energy $E_c = e^2/C_{tot}$ and C_{tot} is approximated as that of a cylindrical capacitor $C_{tot} = \frac{1}{2} ln(L/R)$, L being the length of the nanotube.

Under typical experimental conditions , the contact between the SWNT and the attached (Fermi-liquid) leads is not perfect and the conductance is limited by the electron tunneling into the SWNT which in turn is goverened by the tunnelling density of states. This density is contolled by the parameter g. The boundary conditions will be different depending on how the nanotubes are attached to the probes. If the probe is in contact with a nanotube end then electrons can travel in only one direction, whereas if the probe is in contact with the bulk nanotube the electrons can go in either of two directions. Because of this α_{end} is generally larger than α_{bulk} and the two are given by the formulas

$$\alpha_{end} = \frac{1}{4}(\frac{1}{g} - \frac{1}{4}) \qquad \alpha_{bulk} = \frac{1}{8}(\frac{1}{g} + g - 2) \tag{19}$$

If transport is limited by tunneling through a weak contact from a metal electrode to the SWNT, the full temperature-dependent differential conductance $G(V,T) = dV/dI$ can be evaluated in closed form. If V denotes the voltage drop across the weakest link [5]

$$G(V,T) = AT^{\alpha} cosh(\frac{eV}{2k_BT})|(\Gamma\frac{1+\alpha}{2} + \frac{ieV}{2\pi k_BT})|^2 \tag{20}$$

Where Γ denotes the gamma function and A is a nonuniversal factor depending on the details of the junction. Eqn(13) implies; $T^{-\alpha}G(V,T) = f(\frac{eV}{k_BT})$. All experimental data then for such systems should collapse onto a universal scaling function $f(x)$.

3.1 Experimental Results

The comparison to the theoretical predictions above will now be made using measurements obtained by Egger et al. [3]. In their experiments nanotubes are attached to metallic electrodes and elecrostatic force microscopy (EFM), shown in Fig. [3.1], is used to measure the potential barrier formed at the nanotube/metal interface. This barrier is used to observe the Luttinger liquid behaviour via the tunneling density of states.

The EFM measurement is made by scanning an AFM tip of voltage V_{tip} over a nanotube sample. The electrostatic force between the tip and the sample is given by

$$F_{ac}(w) = \frac{dC}{dz}(V_{tip} + \phi - V_s)^2 \tag{21}$$

The EFM yields a signal that is proportional to the local voltage within the nanotube circuit. However the signal is also proportional to the derivative of the capacitance which will vary as the geometry changes yeilding different signals over a nanotube or a contact at the same potential. To account for this the measurement is taken over the away from the sample edged and should reflect the local voltage within the nanotube.

The results of one set of such experiments is shown in Fig. (3.1). The conductance, G, is plotted as a function of T on a double logarithmic scale for two bulk contacted and two end contacted nanotube ropes. The measured data (solid lines) show approximate power-law scaling behaviour predicted, $G \propto T^{\alpha}$ for the four samples shown. The range of temperatures over which this behaviour occurs is limited by the coulomb blockade effect which is outlined in (4) and corrected for in the dashed curves. Above T 100k, G begins to saturate in some of not all of the samples. The corrected data for bulk contacted samples shows α_{bulk} 0.33 and 0.38 while for end contacted samples α_{end} 0.6 for both samples. The upper inset to the

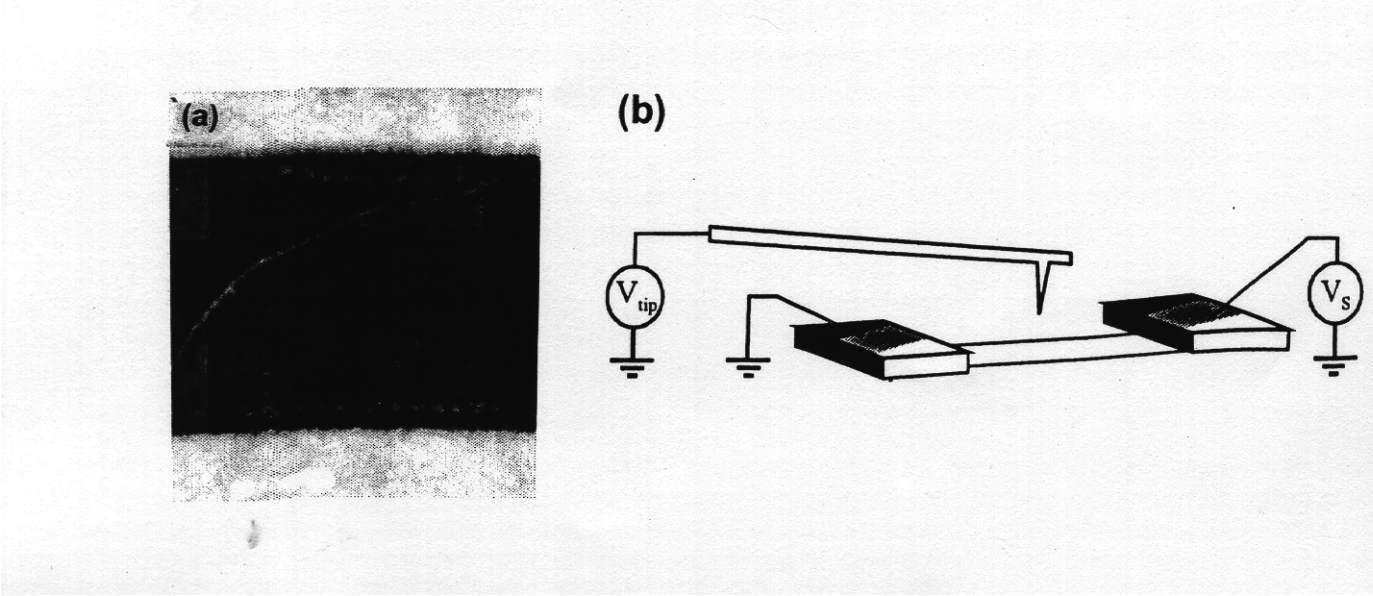

Figure 3: 3a)Topographic AFM image of a 2.5 nm bundle of SWNT's which is seen spanning between two gold electrodes of separation 1μm. b)Experimental setup for ESM [3].

figure the exponents are determined for a variety of samples. Exponents marked with an 'x' are for bulk contacted while the 'o' samples were connected at an end.

In Fig.(3.1) differential conductance is measured as a function of applied voltage at various temperatures in the inset. The plot in the center of the figure demonstrates the existence of the scaled form predicted from Eqn(20).

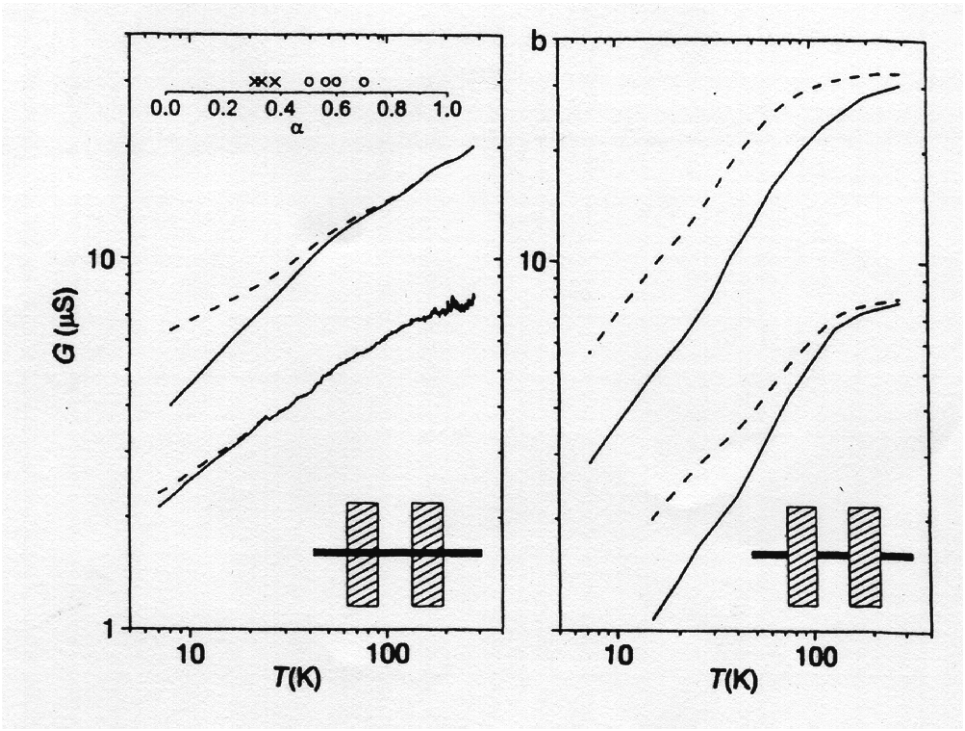

Figure 4: Conductance measured at various temperatures. The left image is for bulk contacted samples and the right for end contacted.

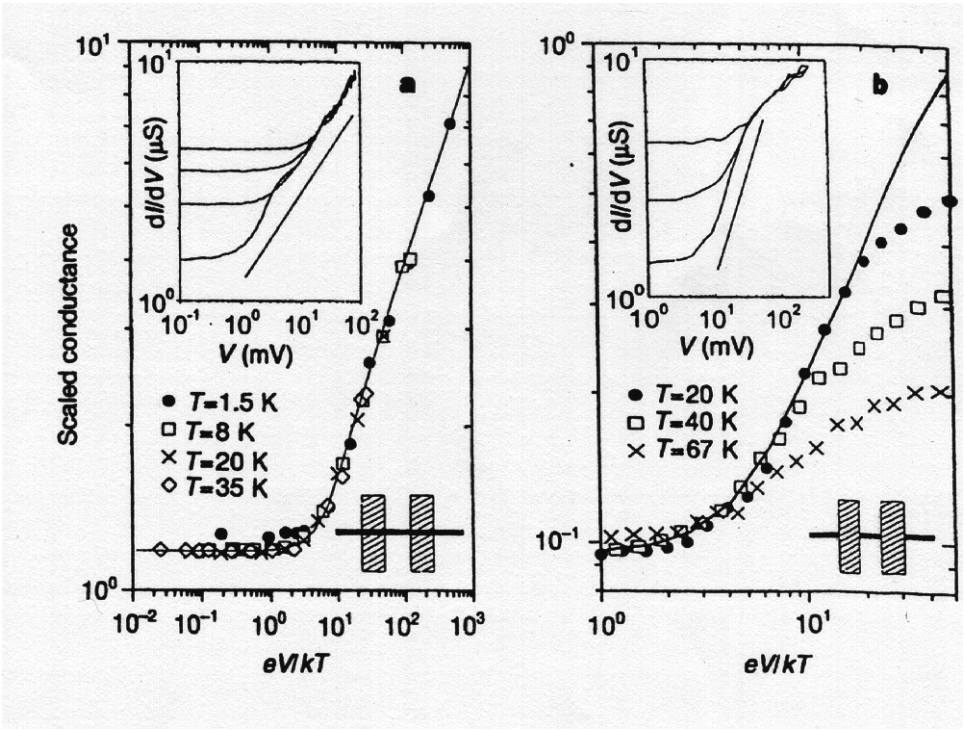

Figure 5: The differential conductance measured at various temperatures. The left image is for bulk contacted samples and the right for end contacted

4 Conclusion

In this paper the basic theory of Luttinger liquids has been outlined. The main properties characterizing Luttinger liquid behaviour were identified as the complete separation of the spin and charge excitations and the power law scaling of Luttinger liquid correlation functions. Luttinger liquids are interesting systems to understand as they are one of the only systems in the field of strongly correlated electrons that can to a large degree be solved analytically. Studying the properties of Luttinger liquids may lead to insight into how to handle higher dimensional systems of strongly correlated electrons a much more difficult problem to even begin treating. In particular the use of bosonization in 1D system has stimulated research into the possibility of extending the technique to higher dimensions.

Experimentally there is strong evidence for the existence of physical Luttinger liquids. The example of carbon nanotubes given above being one such case. The transport properties predicted by the theory have been shown to be in good agreement with the experimental measurements on SWNT. Though some controversy exists as some experiments on SWNT and MWNT support the Luttinger liquid model while others support Fermi liquid behaviour. This discrepency seems to be understood to those working in the field as due to a lack of control over some of the experimental parameters [7] [6].

In an effort to find more conclusive experimental systems attempts were made to find experiments that probed the physical consequences of the complete separation of spin charge excitations. Though some experiments were proposed within the theory literature [2],[3] the physical experiments do not seem to have been preformed at present. Another literature searches on experiments that would be able to demonstrate existence of Luttinger liquid behaviour through a tuning of the interaction terms was made. The idea being that Luttinger liquid behaviour breaks down when $H_{1/3} \neq 0$ (Luttinger liquid model becomes Sine-Gordon model as can see from terms in Fig. 2). Attempts were made to see if any experimental systems exist where there is a way to modulate the dominance of the interaction terms in the Hamiltonian. If the dominance of the umklapp or or backward scattering terms were able to be modulated by some experimental parameter a transition between the two types of behaviour could maybe be observed. For example perhaps tuning the temperature, pressure, sample doping, the presence of transverse electric field or changing the length of the nanotube send the system into different regimes of interaction dominance.

References

[1] David Senechal, http://arXiv:cond-mat/9908262 (1999).

[2] Johannes Voit, http://arXiv:cond-mat/0005114v1 (2000).

[3] R. Egger, A. Bachtold, http://arxiv.org/abs/cond-mat/0008008 (2000).

[4] Marc Bockrath, Thesis Berkeley (1993). http://physics.berkely.edu/research/mceuen/topics/nano

[5] Charles Kane, Pys. Rev.Lett.**79**, 5086 (1997).

[6] Marc Bockrath, David H. Cobden, Jia Lu, Nature **397** (1999).

[7] Laszlo Forro, Christian Schonenberger, Europhysics News **32** No.3